RETROFIT OF MASONRY BUILDINGS WITH CRM - *COMPOSITE REINFORCED MORTAR* - SYSTEM: PRACTICAL DESIGN CONSIDERATIONS ABOUT SEISMIC CAPACITY

Mr Allen Dudine [(1)], Ms Alessia Bez [(1)], Mr Mihel Bosankić [(2)], Mr Pierpaolo Turri [(1)]

[(1)] *Fibre Net S.p.a., Via Jacopo Stellini, 3 - Z.I.U., 33050 Pavia di Udine (UD), Italy*
[(2)] *Röfix d.o.o., Ulica Lusci br. 3, HR-10294 Pojatno, Croatia*

Abstract

Ancient masonry buildings are characterized often by a high seismic vulnerability: innovative intervention strategies for strengthening, based on the use of FRP composite materials are gradually spreading. In particular, the coupling of FRP preformed elements (meshes, angles and connectors) with mortar layers (*Composite Reinforced Mortar* techniques - CRM) evidenced a good physical, chemical and mechanical compatibility with the historical masonry and experimental campaigns proved to be effective for the enhancement of both in-plane and out-of-plane performances of masonry, contrasting the opening of cracks and improving both resistance and ductility. The resistant mechanisms that are created in CRM reinforced masonry walls subjected to in-plane horizontal actions are analyzed in the paper and a practical design approach to evaluate their performances is illustrated, evidencing the dominant collapse mode at the varying of the masonry characteristics. Some masonry walls are analyzed numerically and analytically, as "case study".

Keywords: CRM Reinforcement, existing masonry structures, full-scale experimental test, Composite structures, Glass fibre reinforcement.

1. Introduction

Masonry is one of the most widespread structural systems in Europe for ancient buildings. This principally due to an easy constructions process and due to the availability of materials involved. Since many of these buildings have been realized in the past century, seismic actions have not been considered in the design and, for this reason, structures are dangerously inadequate to resist seismic events. Typical structural weaknesses that can be observed in existing structures are poor lime mortar in masonry joints, irregular or multi-leaf masonry, lack of keying between perpendicular walls or between walls and ceilings and the absence of story diaphragms. The current design challenge is to find a way to make existing structure seismically safer and reduce these deficiencies.

An innovative strengthening technique is the application of the CRM System, namely *Composite Reinforced Mortar*. This system consists of a coupling of FRP preformed elements and a mortar layer. As a first important benefit, the application of this reinforcement allows to reach very high levels of resistance and ductility, often with a negligible impact on the structure stiffness. Furthermore, the system can be effective even when applied on one side only, and for this reason the intervention does not require occupant to move out of their buildings and can represent an effective solution for the ancient structures with architectural or monumental restrictions. To investigate the behaviour of this technology, several studies have been carried out on the CRM System. Gattesco N., Boem I. (2017): Characterization tests of GFRM coating as a strengthening technique for masonry buildings. *Composite Structures*, vol. **165**, 39-52, doi: 10.1016/j.compositesb.2017.07.006.) [1] have carried out several test on CRM elements, to understand the behaviour of the system individually. Moreover, shear compression tests, diagonal compression tests and bending tests on reinforced masonry elements have been developed experimentally and then studied numerically in Gattesco N., Boem I. (2017): Out-of-plane behavior of reinforced masonry walls: Experimental and numerical study. *Composites Part B*, vol. **128**, 209-222, doi: 10.1016/j.compstruct.2017.01.043. [2] and Boem I., Gattesco N. (2021): Rehabilitation of Masonry Buildings with Fibre Reinforced Mortar: Practical Design Considerations

Concerning Seismic Resistance. *Key Engineering Materials*, vol. **898**, 1-7, doi: 10.4028/www.scientific.net/KEM.898.1. [3]. Among all studies, an experimental and numerical analysis on a full-scale masonry building test is missing.

In the present paper, the recent findings about experimental tests on masonry elements (Gattesco N., Rizzi E., Bez A., Dudine A. (2022). Out-of-plane behavior of reinforced masonry walls: Experimental and numerical study, *XIX ANIDIS Conference, Seismic Engineering in Italy*, Turin, Italy. [4]) and on a full-scale test on a masonry building (Gattesco N., Rizzi E., Facconi L., Minelli F., Dudine A. (2022). Investigating the effectiveness of a CRM system: full scale reverse cyclic tests on a two-storey rubblestone masonry building, *XIX ANIDIS Conference, Seismic Engineering in Italy*, Turin, Italy. [5]) are reported. Moreover, several considerations on design approach and an overview of the case studies will be reported.

2. CRM System

The Composite Reinforced Mortar system is a modern reinforcement technology. Modern means that FRP technologies and reinforced mortars replaced the traditional materials like steel and concrete. The modern technologies have the aim to provide the same or better performance with cleaner and faster realization (and lower environmental impact). This system is particularly compatible with masonry.

The reinforcement system consists of a GFRP mesh embedded in a mortar layer. The GFRP (Glass Fiber Reinforced Polimer) mesh is a pre-formed grid composed by horizontal parallel fibers and vertical twisted fibers wires (Fig. 1a), spaced 33 mm, 66 mm or 99 mm. The mortar layer is normally 30-50 mm thick, and it is constituted by a hydraulic lime-based mortar (with a tensile strength determined based on the existing masonry strength). The mortar coating is made effective with a mixed mechanism, by means of adhesiveness and the presence of GFRP connectors.
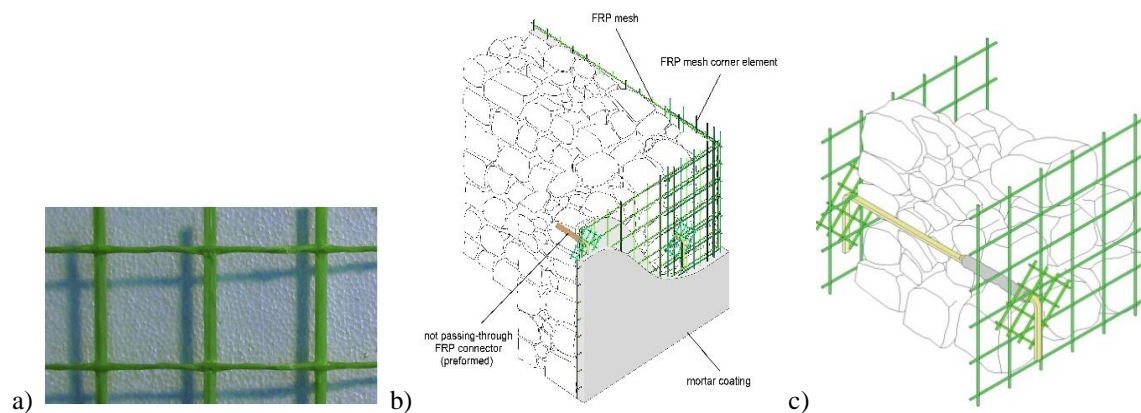

Figure 1. a) GFRP mesh detail (weft wires in vertical direction and warp wires in horizontal direction); b) Fibre Net system application on one side and c) on two sides.

The phases of the system application are briefly reported:

1. Preliminary study of the masonry in its existing conditions (geometry and materials);
2. Removal of eventual existing plasters and scarification of the surface, with high-pressure cleaner;
3. Wetting the masonry surface;
4. Initial stretch coat laying. Under certain conditions, the coat layer is scratched (depending on the conditions of the wall support and mortar characteristics);
5. Prepare the holes for the connectors. The holes, from the diameter of approx. 12 mm, must cross the entire thickness of the masonry so that the two connectors are inserted: a long connector and a short connector. The connectors must overlap inside the hole;
6. Placement of the mesh and insertion of the connectors. In correspondence of the connectors, a stress distributor device must be placed. The stress distributors consist in a GFRP mesh sheet.

7. Placement of the mesh on the other side of the wall, resin injection in the enlarged zone of the hole. Placement of the other stress distributor device and the connector;

8. Application of the mortar coating after the complete hardening of the injected resin, in one or more subsequent layers. The mesh must be placed in the middle of the thickness;

9. Placement of finishing layer and, after the maturing, the paintings and final coverings.

The CRM application allows to achieve higher resistance, because of the mesh which provides tensile strength (otherwise quite low in the unreinforced masonry). Moreover, the system guarantees higher ductility. In fact, the mesh has the capability to confine the cracks and limit their opening.

3. Experimental Campaign

Within the CONSTRAIN project, several experimental tests have been carried out to learn more about the CRM system. As a first step, several tests have been carried out on masonry specimens, on the mortar used for strengthening, on the GFRP mesh in order to investigate on single materials.

3.1 Materials

The stone masonry specimens were realized with rubble limestone blocks. Simple Compression tests carried out on some samples provided average values for the Young's modulus and the compressive strength equal to $E_{masonry}$ = 1074 MPa and $f_{c,masonry}$ = 2.48 MPa, respectively. The experimental tests provided an average compressive strength of the mortar equal to $f_{c,mortar}$ = 0.93 MPa and an average tensile strength of $f_{t,mortar}$ = 0.17 MPa. The brick masonry tests provided $E_{masonry}$ = 2183 MPa and $f_{c,masonry}$ = 6.43 MPa for the double leaves specimens, $E_{masonry}$ = 2341 MPa and $f_{c,masonry}$ = 6.70 MPa for the single leaf specimens.

For the reinforcement, a regular 66x66 mm^2 pattern of the square shape GFRP mesh has been installed. The single parallel wire has a cross section of 11.6 mm^2 and the twisted wire has a cross section of 8.9 mm^2. The GFRP mesh has an average Young's modulus $E_{bar} \geq 25$ GPa, an ultimate characteristic tensile resistance $F_{ub,bar}$ = 4.3 kN and an ultimate tensile strain $\varepsilon_{u,bar}$ = 1.45%. The 30 mm thick mortar coating is based on natural hydraulic lime and has an elastic modulus $E_{mortar} \leq 10$ GPa and a compressive strength at 28 days ageing ≥ 15 MPa. Six L-shaped GFRP elements connectors per m^2 have been placed. Their average ultimate tensile resistance $F_{ub,conn}$ = 21 kN and an average Young's modulus E_{conn} = 21.4 GPa. The distribution GFRP mesh sheets (150x150 mm^2 with mesh dimension 33x33mm^2) have been placed in correspondence of the connectors. Diatons have been also placed, by drilling a 50mm diameter hole and by positioning a steel threaded bar M16, injected with high strength thixotropic mortar.

3.2 Test on Masonry Specimen

Several tests have been made on masonry elements, piers and spandrels, to characterize the behaviour of the entire system. An overview of all the tests carried out is reported below.

Table 1 – Experimental tests overview

Test	Specimen dimension	Masonry type	Reinforcement
Shear compression test on piers	B = 1.50 m H = 1.96 m T = 0.35 m	Double leaves stone masonry - DLSM	NO CRM on one side CRM on two sides
	B = 1.50 m H = 1.96 m T = 0.25 m	Double leaves brick masonry - DLBM	NO CRM on one side CRM on two sides
		Single leaf brick masonry - SLBM	NO CRM on one side
Out-of-plane bending tests on piers	B = 1.03 m H = 2.48 m T = 0.35 m	Single leaf brick masonry	CRM on one side
	B = 1.03 m	Double leaves brick masonry	CRM on one side

| H = 2.48 m T = 0.25 m | Double leaves stone masonry | CRM on one side |

3.2.1 Shear Compression Test

Each specimen was laid over a reinforced concrete element, which is rigidly bounded to the floor. A second reinforced concrete element was placed on the top of the masonry specimens and connected to the steel beam, able to apply both vertical and horizontal forces to the masonry walls. During the tests the out-of-plane displacements were avoided by proper restrain. Firstly, a vertical compression was applied, in order to simulate the loads from the floors (and after that maintained constant during the test). Then, the horizontal force at the top of the specimens was applied to obtain a quasi-static response. The force was varied cyclically in a displacement-controlled test protocol.

Comparing top displacement - applied force trend for the different specimens can give a useful evaluation of the upgrade in resistance provided by the *CRM System*. The trends obtained for the different masonry specimen are reported in Fig. 3.
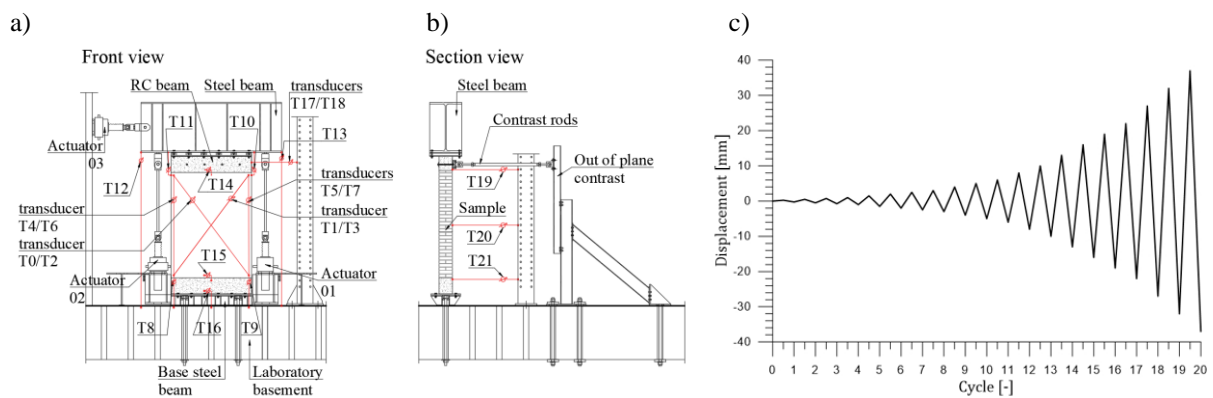

Figure 2. a) Front view of the test setup; b) section view and c) example of a loading time history.
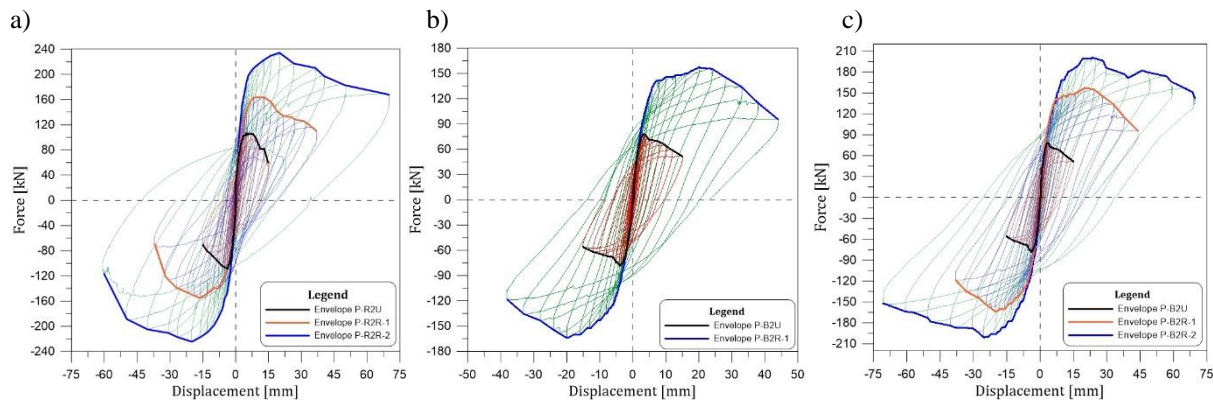

Figure 3. a) Force-displacement trends for DLSM; b) for SLBM; c) for DLBM

Table 2 - Experimental test main results for the shear compression test

Sample	Peak resistance [kN]	Drift at peak resistance [%]	Ultimate Drift [%]
Rubblestone - Unreinforced	107.8	0.24	0.75
Rubblestone – Reinforced on one side	159.5	0.66	1.76
Rubblestone - Reinforced on two sides	229.4	0.99	3.01
Single leaf Brick - Unreinforced	101.9	0.32	0.91
Single leaf Brick – Reinforced on one side	166.4	0.7	1.558
Double leaves Brick - Unreinforced	78.3	0.19	15.03
Double leaves Brick – Reinforced on one side	160.5	1.04	41.12

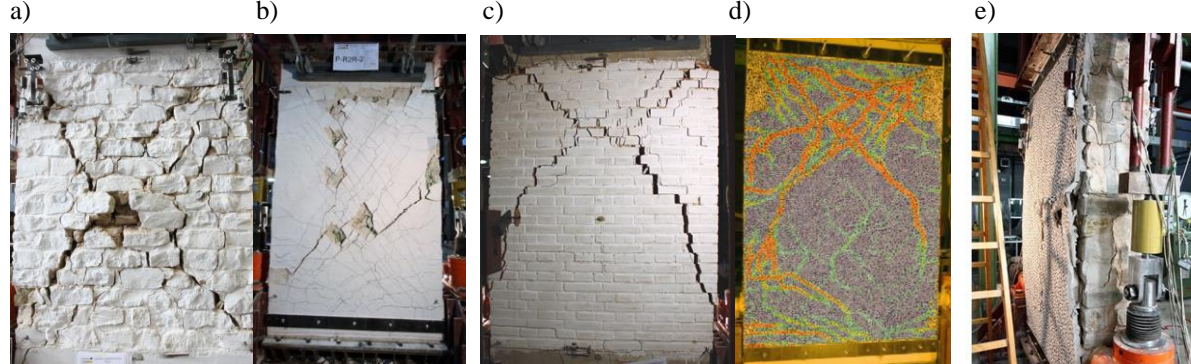| Sample	Peak resistance [kN]	Drift at peak resistance [%]	Ultimate Drift [%]
Double leaves Brick – Reinforced on two sides	201.1	1.24	70.21

a)   b)   c)   d)   e)

Figure 4. Stone masonry specimen at the end of the shear compression test on unreinforced (a) and reinforced (b) side; brick masonry specimen on the unreinforced (c) and reinforced side (d); detachment of the coating (e)

3.2.2 Out of plane Bending Test

Once again in these tests, the specimens were laid over a reinforced concrete element, which was rigidly bounded to the floor both in vertical and in horizontal directions. A second reinforced concrete element was placed on the top of the masonry specimens and connected to the steel structure of the setup structure. Three-point bending tests were carried out by applying a horizontal force at the mid-height section of the specimen and by varying it cyclically in a displacement-controlled test protocol, until a certain damage was reached in the unreinforced side of the wall. The test was then pursued monotonically until failure of the reinforced side. The test setup is reported in Fig.5.
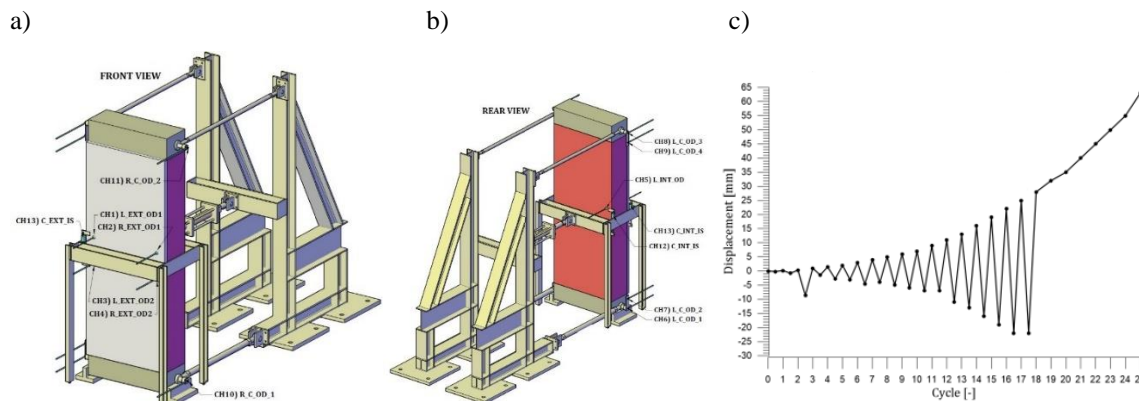
a)   b)   c)

Figure 5. a) Front view of the test setup; b) rear view and c) example of a loading time history.

Comparing top displacement - applied force trend for the unreinforced and reinforced specimens can give a useful evaluation of the upgrade in resistance provided by the *CRM System*. The trends obtained in the different cases are reported in Fig. 5.

Table 3 - Experimental test main results for the three-point bending test

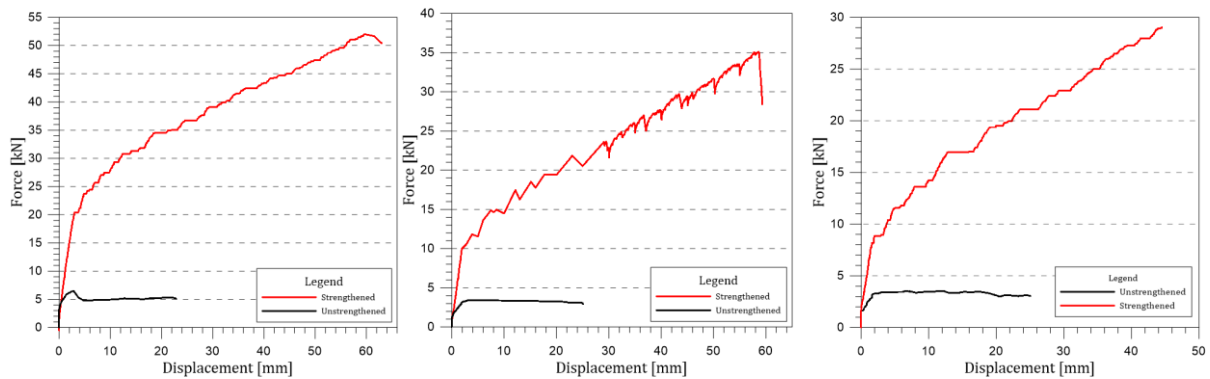| Sample	P_{cr} [kN]	$P_{u(R)}$ [kN]	M_{cr} [kNm]	M_u [kNm]	M_u/M_{cr} [-]	d_{cr} [mm]	d_u [mm]	d_u/d_{cr}
Rubblestone – Double leaves	6.5	52.0	4.4	35.5	8.01	2.81	63.0	22.41
Brick – Single leaf	3.4	35.1	2.3	24.0	10.36	4.31	58.6	13.59
Brick – Double leaves	3.4	29.0	2.3	19.8	8.50	3.13	44.5	14.23

a)   b)   c)

Figure 5. a) Force-displacement trends for rubblestone masonry specimen (unreinforced, reinforced on one side and on two sides); b) Force-displacement trends for single leaf brick masonry specimen (unreinforced, and reinforced on one side); c) Force-displacement trends for double leaves brick masonry specimen (unreinforced, reinforced on one side and on two sides)
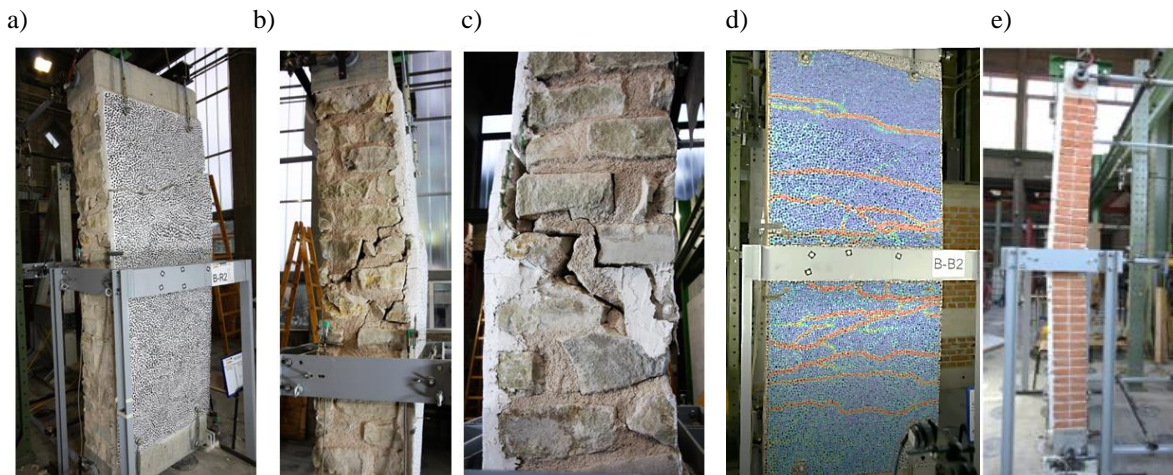

Figure 6. Stone masonry specimen at the end of the bending test on reinforced side (a); detail of the cracks on the specimen (b), (c); brick masonry specimen on the reinforced side (d) and lateral side (e)

3.3 Test on Pilot Building

To conclude the campaign, two experimental tests have been carried on a full-scale building. The structure consists of two-story stone masonry building, composed of four walls (referred to as North, West, South, and East wall), a wooden floor and an ordinary wooden gabled roof. The in-plane dimensions are 5.75 m x 4.35 m, the total height is 6.733 m. The positioning of the openings was design to have different piers aspect ratio, in order to have both shear and flexural collapse mechanisms. During the construction the materials involved were tested and characterized. As can be noted from Fig.7, the loading was applied in the plane of West and East walls (North-South direction) at the first and second story levels, through a vertical stiff steel device connected to the actuator. Load was applied proportionally to the floor mass of every floor level. Vertical loads were applied at floor levels through concrete blocks (first floor) and clay bricks (roof). The structure was strengthened with the *CRM System* on the external side. The reinforcement system was composed by: GFRP mesh with 66x66 mm^2 grid dimension; 30÷40 mm thick mortar coating, L-shaped connectors (4/m^2), 16 mm diameter steel bar which represents the artificial diatons (fixed with thixotropic cement-based mortar and set in the number of 2/m^2); 8 mm steel bars with a fixed spacing had the aim to connect the coating to the concrete foundation.

The behaviors in terms of Base Shear - 2nd story av. lateral displacement are reported below.
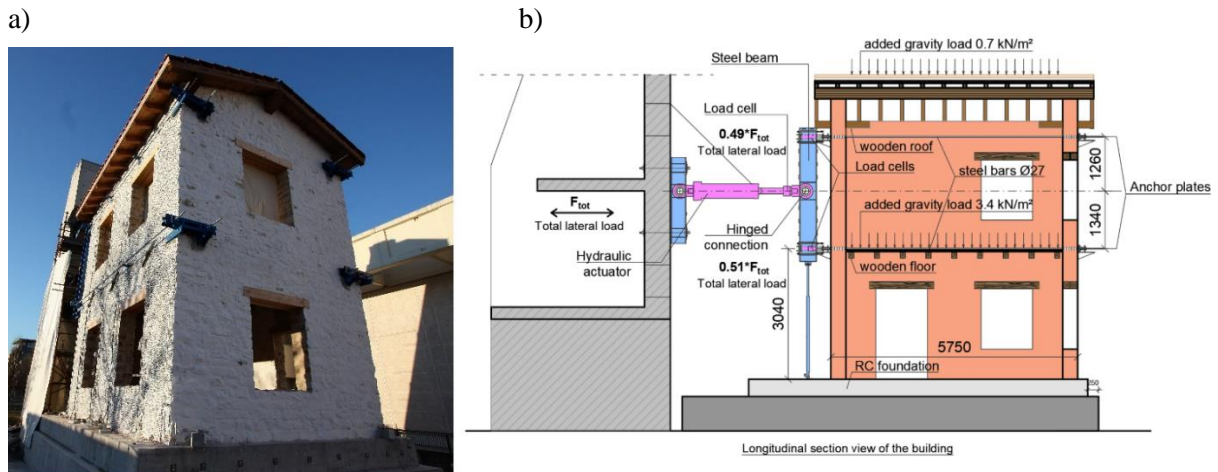
a)   b)

Figure 7. North-East view of the Pilot Building (a); Test setup (b)

The experimental tests give the following results. The crack pattern at the end of the two tests on the East Walls are reported in Fig.9.
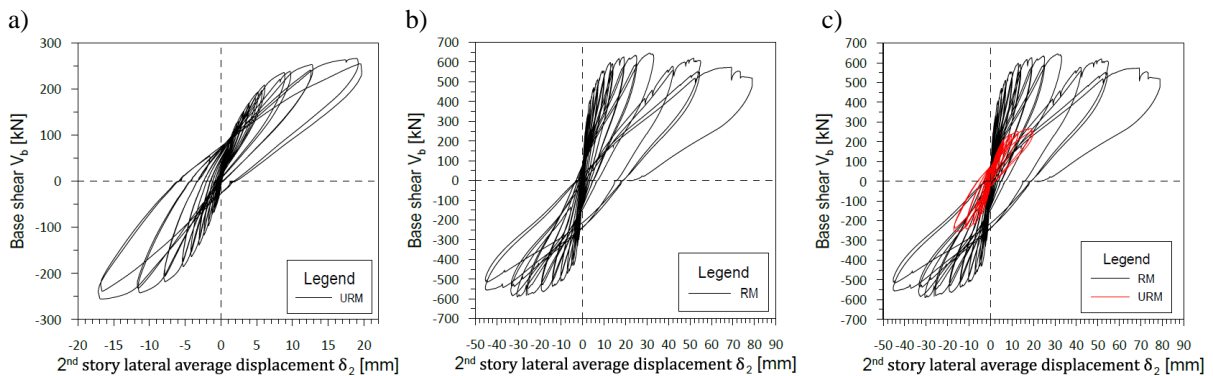

Figure 8. Base Shear – 2nd story displacement curves for the unreinforced building (a), reinforced building (b) and comparison between reinforced and unreinforced behaviors (c)

Table 4 - Experimental test main results for the three-point bending test

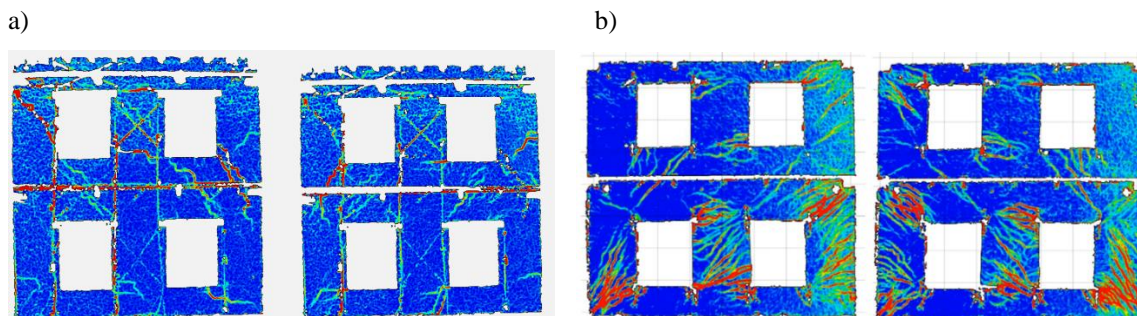| Sample	Load direction	$V_{b,max}$ [kN]	$\delta_{2,max}$ [mm]	$\gamma_{2,max}$ [%]
Unreinforced Building	Positive	267	19.68	0.35%
	Negative	256	17.17	0.30%
Reinforced Building	Positive	645	78.95	1.55%
	Negative	590	45.35	0.89%

a)   b)

Figure 9. Crack pattern on the East wall loaded in negative and positive direction for the unreinforced building (a) and reinforced building (b)

4. Design Formulas

In order to evaluate the improvement provided by the reinforcement system in the practical design, a correct formulation to be used can be the one contained in the CNR DT 215/18 [6]. The relations can be related to the ones valid for the reinforced concrete or the reinforced masonry.
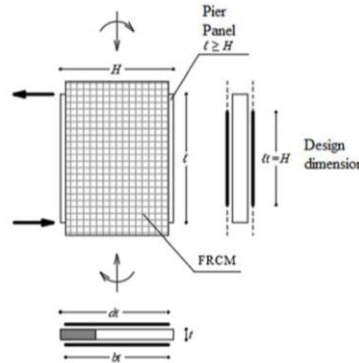

Figure 10. Scheme of a reinforced pier according to [6].

Three cases are considered for the bending resistance of the piers: i) compressive crushing on the compressive edge ($\varepsilon_m = \varepsilon_{mu}$), ii) tensile fracture of mesh ($\varepsilon_f = \varepsilon_{fd}$) and non-linear stress distribution in compression ($\bar{\varepsilon}_m \leq \varepsilon_m \leq \varepsilon_{mu}$), and iii) tensile fracture of mesh ($\varepsilon_f = \varepsilon_{fd}$) and linear stress distribution in compression ($\varepsilon_m \leq \overline{\varepsilon_m}$). The solution is the lowest of the three cases.

For the case i), failure due to compressive crushing of masonry, the equations are:

$$M_{Rd}(N_{Sd}) = f_{md} \cdot \frac{t \cdot y_n}{2} \cdot \left[H \cdot (1-k) - y_n \cdot (1-k)^2 + k \cdot \left(\frac{H}{2} - y_n + \frac{2}{3} \cdot k \cdot y_n \right) \right] + \frac{\varepsilon_{mu}}{y_n} \cdot E_f \cdot t_{2f} \frac{(d_f - y_n)^2}{12} \cdot (2 \cdot y_n + 4 \cdot d_f - 3 \cdot H) \tag{1}$$

$$k = \frac{\bar{\varepsilon}_m}{\varepsilon_{mu}} \tag{2}$$

$$y_n = \frac{N_{Sd} - E_f \cdot t_{2f} \cdot d_f \cdot \varepsilon_{mu} + \sqrt{N_{Sd}^2 + E_f \cdot t_{2f} \cdot d_f \cdot \varepsilon_{mu}[(2-k)t \cdot d_f \cdot f_{md} - 2N_{Sd}]}}{t \cdot f_{md}(2-k) - E_f \cdot t_{2f} \cdot \varepsilon_{mu}} \tag{3}$$

For case ii), failure due to tensile fracture of mesh ($\varepsilon_f = \varepsilon_{fd}$) and non-linear stress distribution in compression ($\bar{\varepsilon}_m \leq \varepsilon_m \leq \varepsilon_{mu}$) the equations are:

$$M_{Rd}(N_{Sd}) = f_{md} \cdot \frac{t}{12} \cdot \left[2 \cdot d_f \cdot y_n \cdot \xi \cdot (2 \cdot \xi + 3) + 3 \cdot H \cdot [y_n \cdot (2 + \xi) - \xi \cdot d_f] - 2 \cdot y_n^2 \cdot (\xi^2 + 3 + 3 \cdot \xi) - 3 \cdot \xi^2 \cdot d_f^2 \right] + \varepsilon_{fd} \cdot E_f \cdot t_{2f} \frac{d_f - y_n}{12} (2 \cdot y_n + 4 \cdot d_f - 3H) \tag{4}$$

$$\xi = \bar{\varepsilon}_m / \varepsilon_{fd} \tag{5}$$

$$y_n = \frac{2 \cdot N_{Sd} + t \cdot \xi \cdot f_{md} \cdot d_f + E_f \cdot t_{2f} \cdot d_f \cdot \varepsilon_{fd}}{t \cdot f_{md}(2 + \xi) + E_f \cdot t_{2f} \cdot \varepsilon_{fd}} \tag{6}$$

Finally, for case iii), tensile fracture of mesh ($\varepsilon_f = \varepsilon_{fd}$) and linear stress distribution in compression ($\varepsilon_m \leq \overline{\varepsilon_m}$) the equations are:

$$M_{Rd}(N_{Sd}) = \frac{t \cdot E_m \cdot \varepsilon_{fd}}{12} \cdot \frac{y_n^2}{d_f - y_n} (3 \cdot H - 2 \cdot y_n) + \varepsilon_{fd} \cdot E_f \cdot t_{2f} \frac{d_f - y_n}{12} (2 \cdot y_n + 4 \cdot d_f - 3 \cdot H) \tag{7}$$

$$y_n = \frac{N_{Sd} + E_f \cdot t_{2f} \cdot d_f \cdot \varepsilon_{fd} - \sqrt{N_{Sd}^2 + E_m \cdot \varepsilon_{fd} \cdot d_f \cdot t \cdot (E_f \cdot t_{2f} \cdot d_f \cdot \varepsilon_{fd} + 2N_{Sd})}}{\varepsilon_{fd} \cdot (E_f \cdot t_{2f} - t \cdot E_m)} \tag{8}$$

For the definition of quantities, it can be useful to refer to the standard. For the shear resistance, the standard refers to the Turnšek - Čačovič formulation as follows:

$$V_{Rd(CRM)} = \frac{1.5 \cdot \tau_{0(R)} \cdot b \cdot t}{\alpha} \cdot \sqrt{\left(1 + \frac{\sigma_0}{1.5 \cdot \tau_{0(R)}}\right)} \tag{9}$$

where $\tau_{0(R)}$ is the equivalent resistance value that takes into account also the reinforced coating:

$$\tau_{0(R)} = \beta \cdot \left(\tau_{0(U)} + m \cdot \frac{t_c}{t} \cdot \frac{f_{t,c}}{1.5}\right) \tag{10}$$

The last part of the project will concern the validation of the analytical formulas proposed by CNR DT 215/2018 [1] with the results obtained in the ongoing experimental tests.

5. Conclusions

The present paper had the principal aim to give an overview of the experimental tests carried out during the project CONSTRAIN, to better understand the role of the CRM System in existing masonry structures. The reinforcement guarantees very good performance, increasing both resistance and ductility. As a practical design advice, the relations to be used are reported in the paper, these relations provided consistent results with the experimental findings. All these considerations can be very useful to further improve the CRM System.

Acknowledgements

References

[1] Gattesco N., Boem I. (2017): Characterization tests of GFRM coating as a strengthening technique for masonry buildings. *Composite Structures*, vol. **165**, 39-52, doi: 10.1016/j.compositesb.2017.07.006.

[2] Gattesco N., Boem I. (2017): Out-of-plane behavior of reinforced masonry walls: Experimental and numerical study. *Composites Part B*, vol. **128**, 209-222, doi: 10.1016/j.compstruct.2017.01.043.

[3] Boem I., Gattesco N. (2021): Rehabilitation of Masonry Buildings with Fibre Reinforced Mortar: Practical Design Considerations Concerning Seismic Resistance. *Key Engineering Materials*, vol. **898**, 1-7, doi: 10.4028/www.scientific.net/KEM.898.1.

[4] Gattesco N., Rizzi E., Bez A., Dudine A. (2022). Out-of-plane behavior of reinforced masonry walls: Experimental and numerical study, *XIX ANIDIS Conference, Seismic Engineering in Italy*, Turin, Italy.

[5] Gattesco N., Rizzi E., Facconi L., Minelli F., Dudine A. (2022). Investigating the effectiveness of a CRM system: full scale reverse cyclic tests on a two-storey rubblestone masonry building, *XIX ANIDIS Conference, Seismic Engineering in Italy*, Turin, Italy.

[6] CNR DT 215/2018 (2020) 'Guide for the Design and Construction of Externally Bonded Fibre Reinforced Inorganic Matrix Systems for Strengthening Existing Structures'. National research Council, Rome, Italy.